

Article

Corrosion of Metals Modified with Formulations Based on Organosilanes

Maxim Petrunin * , Tatyana Yurasova, Alevtina Rybkina  and Liudmila Maksaeva

Frumkin Institute of Physical Chemistry and Electrochemistry, Russian Academy of Sciences, Moscow 119071, Russia; lmaksaeva@mail.ru (L.M.)

* Correspondence: mmvp@bk.ru

Abstract: Methods for preliminary modification of the surface of structural metals with formulations based on organosilanes, including both solutions of individual organosilanes and two-component mixtures consisting of two organosilanes or an organosilane with an organic corrosion inhibitor, have been developed. As a result of this modification, a self-assembling siloxane polymeric/oligomeric nanoscale layer is formed on the metal surface. Such layers are capable of changing the physico-chemical properties of the metal surface, in particular reducing the susceptibility of the metal to corrosive destruction. In this work, the mechanism of formation of organosilicon nanolayers and their effect on the electrochemical and corrosion behavior of metals have been studied in detail by a set of electrochemical methods, while laboratory studies and accelerated corrosion tests of carbon steel and zinc, modified with formulations based on organosilanes, have been carried out. The greatest inhibitory effect is demonstrated by two-component modifying formulations, namely mixtures of vinyl with aminosilane and vinylsilane with benzotriazole. The mechanism of corrosion inhibition by surface nanolayers formed upon surface modification with two-component mixtures has been considered.

Keywords: metal corrosion; organosilanes; surface modification; self-assembled siloxane layers; corrosion inhibition full-scale natural corrosion tests; electrochemical impedance spectroscopy



Citation: Petrunin, M.; Yurasova, T.; Rybkina, A.; Maksaeva, L. Corrosion of Metals Modified with Formulations Based on Organosilanes. *Metals* **2023**, *13*, 721. <https://doi.org/10.3390/met13040721>

Academic Editor: Shidong Wang

Received: 28 February 2023

Revised: 3 April 2023

Accepted: 4 April 2023

Published: 6 April 2023



Copyright: © 2023 by the authors. Licensee MDPI, Basel, Switzerland. This article is an open access article distributed under the terms and conditions of the Creative Commons Attribution (CC BY) license (<https://creativecommons.org/licenses/by/4.0/>).

1. Introduction

Despite significant progress in the development of new materials, metals used by humankind for centuries still remain the main structural materials in various fields of industry. However, despite all their advantages, metals have a significant drawback: they are degraded by the environment, i.e., they are subject to corrosion. That is why, throughout human history, in parallel with the development of new methods for manufacturing a wide range of items made of structural metals, significant efforts at elaborating ways to reduce corrosion losses were undertaken. Corrosion protection is one of the oldest scientific and technical problems. Numerous textbooks, scientific collections and scientific periodicals published in various countries deal with metal corrosion and ways to prevent it. However, despite the intense studies, no versatile methods have been suggested so far to prevent or significantly reduce the corrosion losses of metals, and corrosion remains one of the most serious problems confronting modern industry. Currently, the problem of reducing corrosion losses of metal structures is becoming more and more acute in industrially advanced countries, since the annual costs of corrosion protection in developed countries amount to huge sums of billions of dollars [1–4]. Corrosion can cause direct and indirect costs that can reach up to 6% of a country's gross domestic product [5]. In addition to direct and indirect costs, huge amounts of metals are irreparably lost due to corrosion. According to the estimates of the US National Bureau of Standards, in the 1980s in the United States about 40% of the metal produced annually was spent on the replenishment of corrosion losses. Such huge losses can be reduced, since it is believed [2] that the use

of advanced anticorrosion technologies and approaches (for example, the use of modern insulation coatings) can reduce corrosion costs and metal losses by ca. 20–25%. In addition, environmental safety issues of various industries have become of paramount importance in recent decades [6]. The relationship between the problems of corrosion safety and environmental safety is obvious since the failure of metal structures is often accompanied by severe ecological consequences; for example, ingress of petroleum products or chemicals into the natural environment when the integrity and impermeability of product pipelines are lost or explosions occur during accidents on oil and gas pipelines. One of the ways to improve environmental safety is to reduce the pollution of the environment with toxic metals, since in recent years metal corrosion has been considered one of the ways of dispersing metals into the environment where they can adversely affect ecological systems. Along with mercury, cadmium and lead, which are toxic to living organisms, ecological concern regarding metals such as copper, zinc and aluminum has also increased [7,8]. In this regard, despite the long-term interest of researchers, the development of ways to prevent and reduce corrosion is a very urgent scientific and technical problem, both from the economic and environmental points of view.

Polymer and paint coatings have been successfully used for many years as one of the most efficient means to reduce corrosion hazards during the operation of metal structures and buildings under various conditions [9]. Usually, chemical pretreatment of the metal surface is performed to increase corrosion resistance and improve coating-metal adhesion. Typically, solutions of hexavalent chromium compounds are used as pretreatment compounds that form conversion coatings consisting of chromate-containing coating layers on the metal surface. Chromate layers efficiently protect the metal from corrosion and provide the coating with high adhesion; however, hexavalent chromium compounds are toxic, and in particular, they have a carcinogenic effect. The use of chromate coatings is prohibited in the EU, but many countries still use technologies that involve chromates. In recent decades, the efforts of researchers have been aimed at replacing chromate technologies [10–14]. However, the suggested replacement methods are either less efficient or do not comply with the modern principles of environmental safety. Thus, no methods of surface pretreatment alternative to chromates that would provide adequate anticorrosive and adhesive characteristics have been suggested so far.

One of the promising ways to increase interphase interaction at the metal–polymer interface is to create an additional intermediate layer on the substrate surface before the latter contacts an adhesive [15]. Compounds capable of forming such layers are called adhesion promoters. Organic adhesion promoters include organotitanates, organocirconates, benzotriazoles, etc. [16]. Among these, organosilicon adhesion promoters stand out for their unique properties [17–21]. A special feature of these compounds is manifested in the versatility of the promoting effect on substrates and polymers of various types. Organic silanes (organosilanes or silanes) with the general formula $R_nSi(OR')_{4-n}$ are compounds that can be adsorbed onto the metal surface and, due to their multifunctionality, and at the same time, form strong and hydrolytically stable Me–O–Si bonds with the hydroxylated surface of an inorganic material (metal), can polymerize with formation of self-organizing layers, and can react with the components of a wide range of polymer coatings. Such layers can change the properties of the surface, in particular inhibiting corrosion [17,19]. It is believed [11] that organosilicon surface layers obtained upon adsorption of organosilanes on a metal can replace toxic chromate coatings that are prohibited from use. In view of the above, it may be expected that such surface layers would prevent the corrosion of metals. As a result of the modification of the metal surface with compositions based on organosilanes, surface layers are formed on it, consisting of polymer/oligomeric siloxane molecules, the units of which are bonded: with the surface by strong covalent bonds Me–O–Si, and between themselves, siloxane bonds Si–O–Si. Neighboring polymer molecules are also linked by cross-siloxane bonds Si–O–Si [17,19]. When using a mixture of organosilane with benzotriazole for modification, instead of siloxane polymeric molecules, a layer of polymeric siloxane-azole molecules is formed on the surface, in which both units in each

molecule and neighboring molecules are interconnected not only by siloxane (Si-O-Si-), but also additional silazane (Si-N-C-) bonds. Due to this, a more densely cross-linked surface layer is formed! The purpose of this work was to study the effect of organosilicon surface layers on the corrosion behavior of metals.

2. Materials and Methods

The following metal materials were used in this work: cold-rolled carbon steel (grade 08ps, 0.05–0.11% C), zinc (grade Ts0, 99.975% Zn). Samples made of 08kp steel (carbon content 0.05 wt.%, thickness 100 μm) with a contact plate (3 mm \times 40 mm) were used for electrochemical and corrosion studies (Figure 1). The working area of the samples was 2.5 cm². Preliminary preparation of samples before exposure included mechanical surface cleaning on a grinding machine (P1000 sandpaper, abrasive cloth with a grain size of 14–20 μm) and degreasing with ethanol. Table 1 shows the compounds used in this work to modify the surface of metals, and Table 2 shows the composition of the modifying solutions. Modification of the surface of samples was performed by immersing whole metal plates in aqueous or organic (Table 2) solutions of modifiers for 10 min. After modification, a sample was immersed in a solvent for 1 min to remove the excess modifier, then the samples were dried in air. Both one- and two-component systems were used in this work. The one-component systems included: 1% VS, 3% VS, 1% AS, and 2% AS solutions in water; 1% MS, 1 mM BTA, and 10 mM BTA solutions in ethyl alcohol. The two-component systems included: a solution of the (1% VS + 1% AS) mixture in water; and a solution of the (1% VS + 1 mM BTA) mixture in ethyl alcohol.

Electrochemical studies were carried out in a borate buffer solution (0.4 M H₃BO₃ + 5.5 mM Na₂B₄O₇ \times 10H₂O, pH 6.7) with the addition of 0.1 M NaCl.

The borate buffer solution was used in order to exclude the influence of changes in the near-electrode pH on the kinetics of the corrosion process, since it is known [22] that the reactions accompanying metal corrosion change the acidity of the solution, namely: the hydrolysis of metal ions released in the anodic process of corrosion dissolution leads to acidification of the solution, and the cathodic reaction of oxygen ionization leads to its alkalization. In addition, it is known [23,24] that borate ions, unlike other electrolyte anions, do not participate in the process of iron ionization; therefore, the borate buffer solution is often used as a background electrolyte when conducting corrosion and electrochemical studies [23–27].

Table 1. Modifier compounds used in the study.

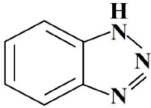
No.	Conventional Abbreviation	Name	Chemical Formula
1	VS	Vinyltrimethoxysilane	CH ₂ =CH-Si(OC ₂ H ₅) ₃
2	AS	γ -Aminopropyltriethoxysilane	NH ₂ (CH ₂) ₃ -Si(OC ₂ H ₅) ₃
3	DAS	Aminoethylaminopropyltrimethoxysilane-diaminsilane-diaminosilane	NH ₂ -CH ₂ -CH ₂ -NH-CH ₂ -CH ₂ -CH ₂ -Si(OCH ₃) ₃
4	GS	γ -Glycidoxypropyltriethoxysilane	CH ₂ -(O)CH-CH ₂ -O-(CH ₂) ₃ Si(OC ₂ H ₅) ₃
5	MS	γ -Methacryloxypropyltriethoxysilane	CH ₂ =C(CH ₃)-C(O)-O-CH ₂ -CH ₂ -Si(OC ₂ H ₅) ₃
6	BTA	1,2,3-benzotriazole	

Table 2. Composition of solutions used to modify the surface of metal samples.

No.	Modifier Compounds		Solvent
	First Component	Second Component	
1	0.01% VS	-	Water, pH 6.9
2	0.1% VS	-	Water, pH 6.9
3	1% VS	-	Water, pH 6.9
4	2% VS	-	Water, pH 6.9
5	3% VS	-	Water, pH 6.9
6	5% VS	-	Water, pH 6.9
7	0.01% AS	-	Water, pH 6.9
8	0.1% AS	-	Water, pH 6.9
9	1% AS	-	Water, pH 6.9
10	2% AS	-	Water, pH 6.9
11	1% DAS	-	Water, pH 6.9
12	1 mM BTA	-	Water, pH 6.9
13	10 mM BTA	-	Water, pH 6.9
14	1% MC	-	C ₂ H ₅ OH
15	1% VS	1% AS	Water, pH 6.9
16	1% VS	1 mM BTA	C ₂ H ₅ OH
17	1% VS	10 mM BTA	C ₂ H ₅ OH
18	1% GS	-	Water, pH 6.9
19	5% GS	-	(Water with addition of acetic acid), pH 4.0

**Figure 1.** Photograph of a metal sample for electrochemical testing.

Electrochemical measurements were carried out in a standard three-electrode cell using an IPC-Pro MF potentiostat (“Volta”, Saint Petersburg, Russia). After grinding with grade “0” sandpaper, the samples were additionally washed in a “Sapphire—0.8 TTs” ultrasonic bath in a C₂H₅OH:C₇H₈ (1:1) mixture for 25 min. In order to eliminate the edge effects at the ends of the sample, after modification and air drying for 120 min, the sample was coated with a chemically resistant varnish, leaving an “open window” so that the working surface area of the electrode was 1 cm². Measurements were carried out in a 0.1 M NaCl solution (100 cm³). The pH was stabilized by the addition of borate buffer solution (0.4 M H₃BO₃ + 5.5 mM Na₂B₄O₇ × 10H₂O, pH 6.7). A platinum electrode with an area

of 1.2 cm² was used as the auxiliary electrode, and a silver chloride electrode was used as the reference electrode. The measured potentials were converted to the normal hydrogen electrode (NHE) scale.

For the first 300 s after the sample was immersed in the solution, its corrosion potential (E_{cor}) was recorded. This time was sufficient to stabilize the E_{cor} value. Next, anodic potentiodynamic polarization curves were recorded at a scan rate of 0.1 mV/s from this value to the potentials corresponding to the local anodic dissolution at a stationary rate of pit growth on the metal surface. Once the polarization curves were recorded, polarization was switched off and the E_{cor} value was recorded after 60 s, until full stabilization of this parameter was achieved (so that it did not change more quickly than by 0.05 mV/min). In addition to the anodic curves, the kinetics of the change in the anodic current under potentiostatic polarization was determined (at a constant anode potential $E_{\text{an}} = 0.2$ V (NHE)). The variation in the state of the sample surface was recorded by in situ optical microscopy in parallel with the electrochemical measurements. The following equipment was used: a Biomed PR-3 microscope with 5 \times magnification (visible sample area $S_{\text{vis}} = 1.00$ mm²), 10 \times ($S_{\text{vis}} = 0.5$ mm²) and 20 \times ($S_{\text{vis}} = 0.25$ mm²) with a connected Amoyca AC-300 digital video camera. The camera resolution was 2048 \times 1536 pixels. The data from the camera were transmitted to a computer and processed in the ScopePhoto 3.0 program.

Electrochemical impedance spectroscopy (EIS) was used to estimate the effect of surface modification of carbon steel on its corrosion behavior. EIS measurements were carried out using an electrochemical set-up based on an IPC-Pro MF potentiostat with an FRA module ("Volta", Saint Petersburg, Russia). The method involves testing samples by alternating voltage (potential) with recording the value of alternating current response and the phase shift and amplitude changes in the range of the frequencies used. Figure 2 shows the layout of the electrochemical cell for EIS studies. The measurements were carried out in the frequency range from 10 kHz to 0.1 Hz with an alternating voltage amplitude (ΔE) of 10 mV at the open circuit potential.

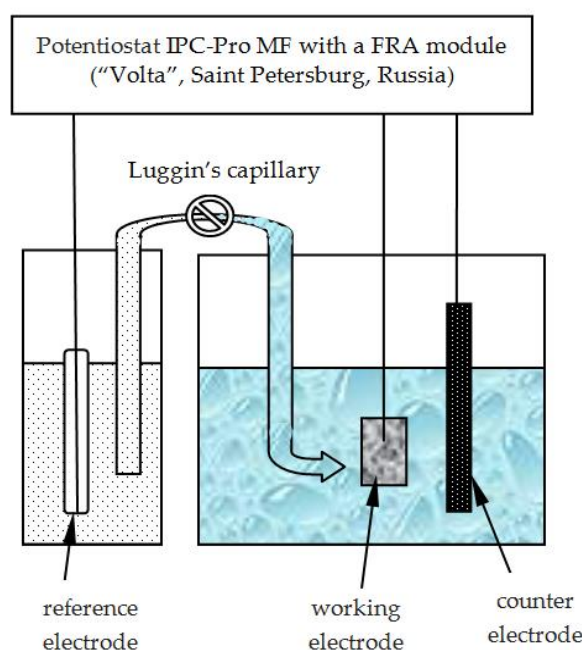


Figure 2. Layout of the electrochemical cell for EIS studies.

The conducted EIS studies make it possible to determine the characteristics of the metal's corrosive behavior by estimating the values of the elements (for example, resistance, capacitance, etc.) of an equivalent circuit describing the parameters of the sample under study, taking into account the reactions occurring on the sample in the working electrolyte. During the tests, the data required to assess the corrosion behavior of the

metal were recorded automatically. The parameters of an equivalent circuit adequately simulating experimental impedance spectra were calculated using the DCS program [28]. A detailed description of equivalent electrical circuits used to simulate the processes occurring in the systems under study will be considered below. Borate buffer solution (0.4 M H_3BO_3 + 5.5 mM $\text{Na}_2\text{B}_4\text{O}_7 \times 10\text{H}_2\text{O}$, pH 6.7 additionally containing 0.1 M NaCl) was used as the working electrolyte. Accelerated tests in an electrolyte and in an atmosphere were performed using rectangular samples made of grade Ts0 zinc with dimensions 10 mm \times 50 mm \times 0.8 mm. The tests were carried out in a borate buffer solution (composition: 0.4 M H_3BO_3 + 5.5 mM $\text{Na}_2\text{B}_4\text{O}_7 \times 10\text{H}_2\text{O}$, pH 6.7) with NaCl added to a concentration of 0.1 M. Accelerated tests in an atmosphere were performed in a Terchy MHK-408CL climate chamber (manufactured by TERCHY Environmental Technology LTD, Taiwan) at $t = 60^\circ\text{C}$ and RH = 95%. The duration of the tests was 51 days.

The corrosion rate was estimated by the gravimetric method by weighing the samples before and after the tests. Before the tests, the samples were polished with "0" grade sandpaper, washed with distilled water, dried, degreased with ethyl alcohol, and weighed on an AF-R220CE electronic analytical balance. At the end of the corrosion tests, corrosion products were removed from the metal surface by the standard etching method [29], after which it was reweighed. The weight loss of samples per area unit (Δm), g/cm², was calculated using Equation (1):

$$\Delta m = \frac{m_0 - m_1}{S} \quad (1)$$

where m_0 is the sample weight before the test, g;

m_1 is the sample weight after the test and removal of the corrosion products, g;

S is the sample surface area, cm².

Three samples were exposed in parallel and the arithmetic mean of the weight loss was calculated for each modifying system.

Next, the weight loss was converted to the change in thickness (ΔL), mm, using Equation (2):

$$\Delta L = \frac{\Delta m}{\rho} \quad (2)$$

where ρ is the metal density, g/cm³.

Further, the corrosion rate of steel k was determined in mm/day (Equation (3)) or in mm/year (Equation (4)):

$$k = \Delta L / \tau \quad (3)$$

$$k = (\Delta L / \tau) \times 365 \quad (4)$$

where τ is the test duration, days.

The critical pitting potential (E_{pit}), i.e., the potential above which pitting dissolution of the metal occurs and stable pits are formed [30], was determined from the anodic polarization curves as a breakpoint on the curve (the potential after which a sharp increase of the current is observed) [30,31].

The change in the electrode pitting potential (E_{pit}) to more positive values was chosen as a criterion for the inhibition efficiency of local anodic dissolution after the modification of the metal surface (Equation (5)) [32]:

$$\Delta E = E_{pit} - E_{pit}^{\text{mod}} \quad (5)$$

where E_{pit} is the critical pitting potential of the non-modified metal and E_{pit}^{mod} is that of the modified metal.

The efficiency of corrosion inhibition was estimated using the corrosion inhibition coefficient (Equation (6)) [33,34]:

$$\gamma = K_0 / K_{\text{mod}} \quad (6)$$

where K_0 is the corrosion value (corrosion rate) of the non-modified metal and K_{mod} is the corrosion value (corrosion rate) of the metal after surface modification.

The number of pits was determined using image processing with a computer program Pitting 1.0, developed at our institute specifically for such studies. In some cases, the accuracy of the program was checked by manually counting the pits. Given that the dimensions of the test samples are the same, the figures show the number of pits per sample—on the one hand, the changes in which were recorded by a video camera. The reverse side of the sample was insulated with a chemically resistant varnish. Three samples were examined in parallel; the discrepancy between the samples did not exceed 1 pitting. The corresponding figures show the average number of pits for 3 samples.

3. Results and Discussion

The electrochemical behavior of carbon steel modified with formulations based on organosilanes was studied. Anodic polarization curves were obtained. In Figure 3, curve 1 is the anodic curve of non-modified steel. It can be seen from Figure 3 that the shape of the curve matches the classical shape of curves for passivating metals [35,36].

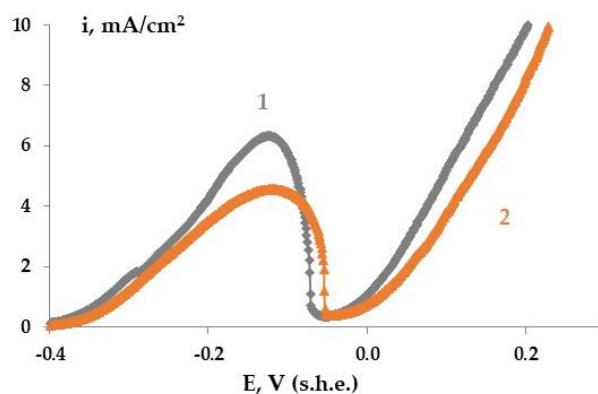


Figure 3. Anodic polarization potentiodynamic curve of St3 carbon steel in 0.1 M NaCl solution: 1—non-modified steel, 2—steel pre-modified with a VS solution. Potential scan rate: 1 mV/s.

The following parts are observed in curve 1 (Figure 3): a pronounced section of active-passive transition in the range of potentials from -0.34 to -0.06 V, a section corresponding to the passivity of the metal with a full passivation potential equal to -0.06 V, a short section corresponding to the passive state, a violation of the passive state (with a critical potential of pit formation E_{pit} approximately equal to $+0.02$ V) and a section corresponding to pitting dissolution at potentials more positive than E_{pit} .

Obtaining polarization curves for all modifying compositions showed that modification with AC solution has practically no effect on the anodic curve of unmodified steel.

Surface modification with the (VS + AS) mixture leads to a decrease in the critical passivation current i_p (current value at the peak of the curve) to 4.2 mA/cm². For unmodified steel and steel modified with VS, the value of i_p was 6.29 and 4.55 , respectively (Figure 3, curves 1 and 2). In addition, a positive shift of E_{pit} by 70 mV was also observed. For the VS solution, this was 55 mV. The use of the modifying mixture (VS + BTA) provided a decrease in i_p to $3/8$ mA/cm² and an increase in E_{pit} by 78 mV. This indicates inhibition of both uniform (reduction of i_p) and local (increase of E_{pit}) anodic dissolution of the steel by the surface layers.

In addition to steel, the electrochemical behavior of zinc was studied (Figures 4 and 5) and it was shown that an increase in potential (when obtaining an anode curve) leads to pitting dissolution of the metal (Figure 5a).

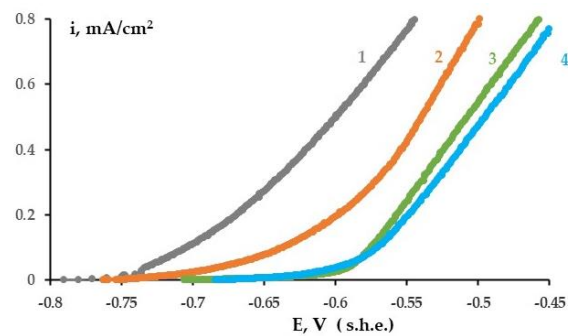


Figure 4. Anodic polarization curve of zinc. 1—non-modified zinc, 2—zinc modified with a VS solution, 3—zinc modified with a solution of a (VS + AS) mixture, 4—zinc modified with a solution of a (VS + BTA) mixture.

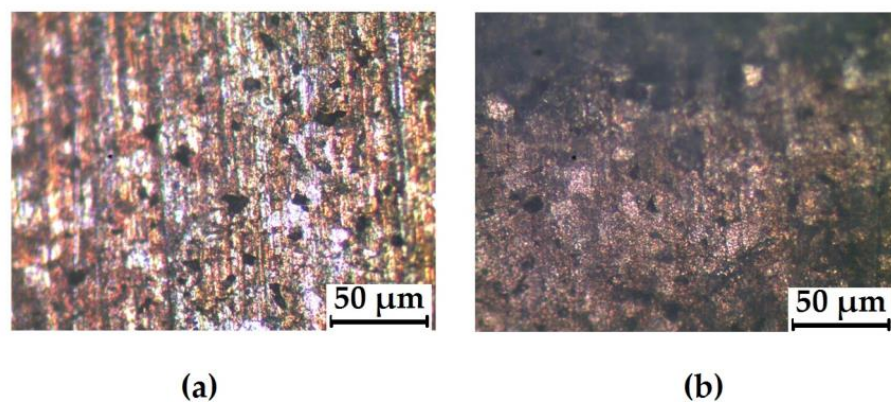


Figure 5. Zinc surface after taking the anodic polarization curve, (a) non-modified zinc; (b) zinc modified with a VS solution.

Figure 4 shows the anodic polarization curve of unmodified zinc and zinc coated with organosilicon layers; the table shows the effect of modification on the value of E_{pit} . From Figure 4 and Table 3 it can be seen that the surface organosilicon layer inhibits anodic zinc dissolution and shifts E_{pit} to the positive side (i.e., inhibits pitting zinc dissolution). For example, in the case of surface modification with VS solution, a smaller number of pits and a smaller size were found on the surface (Figure 5b) than in the case of unmodified metal (Figure 5a). The anodic dissolution of zinc is most effective with modification by mixtures: (VS + AS) (Figure 4, curve 3) and (VS + BTA) (Figure 4, curve 4).

Table 3. The effect of zinc surface modification on the value of pitting potential.

NN-Sequence Line Number	Systems	E_{pit} , V (s.h.e.)	ΔE , V
1	Zn	−0.934	0
2	Zn + VS	−0.84	0.094
3	Zn + (VS + AS)	−0.793	0.141
4	Zn + (VS + BTA)	−0.784	0.15

Observations of the state of metal surface and recording the changes under an optical microscope were carried out in parallel with electrochemical measurements. Figure 6 shows the photographs of steel surface taken at various anodic potentials corresponding to the potentials on the anodic curve (Figure 3, curve 1).

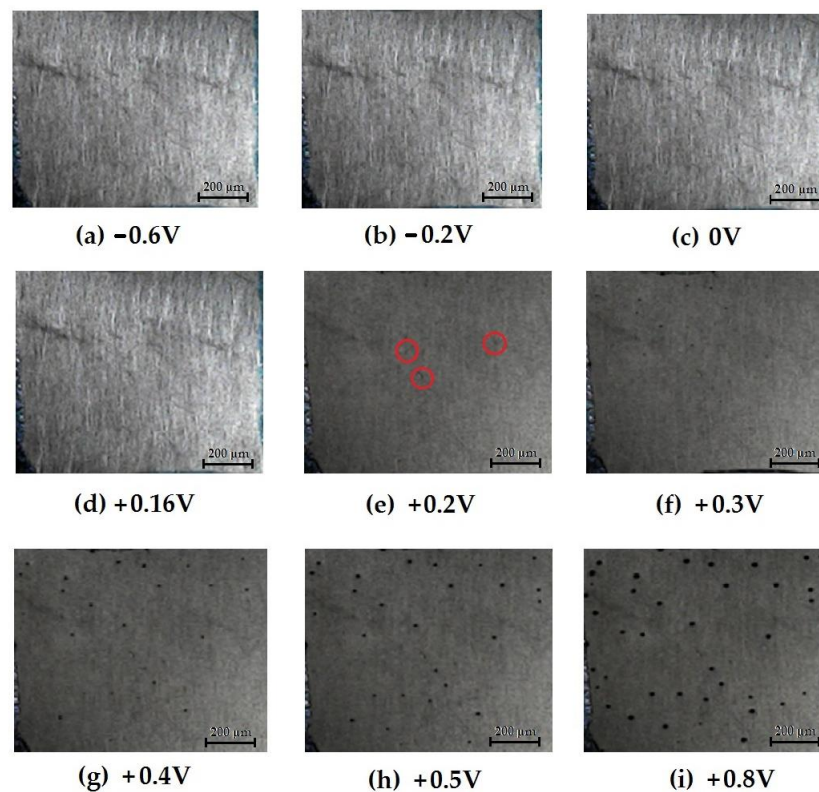


Figure 6. Change in the state of carbon steel surface during anodic polarization of the metal at potentials of: (a) -0.6 V; (b) -0.2 V; (c) 0 V; (d) $+0.16$ V; (e) $+0.2$ V; (f) $+0.3$ V; (g) $+0.4$ V; (h) $+0.5$ V; (i) $+0.8$ V.

In Figure 6 it can be seen that as the potential was varied in the range from -0.6 V to $+0.16$ V (Figure 6a–d), the appearance of the metal surface nearly did not change. As expected, no pitting was detected on the surface until the critical potential of pit formation was reached. Moreover, shifting the potential in the positive direction from the E_{pit} did not cause an instant formation of pits, either. Despite the fact that the potential was shifted to a value more positive by 100 mV than E_{pit} , no pits were detected on the surface (Figure 6d). The first defects detected under the microscope appeared when the potential reached $+0.2$ V (Figure 6e). A further increase in the potential (above $+0.2$ V) led to intensification of the pitting dissolution of metal, which manifested itself both in an increase in the density of the metal dissolution current (Figure 3, curve 1) and in the growth of the number of pits (Figures 6f–h and 7, curve 1). Preliminary modification of a steel surface with formulations based on organosilanes affected the electrochemical behavior of the metal. Thus, modification of the surface with a VS solution resulted in a slight decrease in the critical passivation current (from 6.2 to 4.55 mA/cm²) (Figure 3, curve 2), which can indicate an increase in metal passivation in the presence of a vinylsiloxane nanolayer on the surface and, as a consequence, inhibition of uniform dissolution (corrosion) of the metal. The shift in the pit formation potential in the positive direction (by 70 mV) indicates that the metal pitting dissolution is inhibited. Thus, analysis of anodic electrochemical and optical data showed that the preliminary modification of the steel surface with a vinyl-containing silane should inhibit both uniform and local corrosion of carbon steel. As the potential increases to $+0.8$ V, both the number and the size of pits change. In fact, the pits that appeared on the metal during polarization in the potential range from -0.05 to $+0.5$ V had a visible diameter of about 0.1 mm, while the diameter of the pits that formed at $+0.8$ V was up to 0.25 mm (Figure 6i).

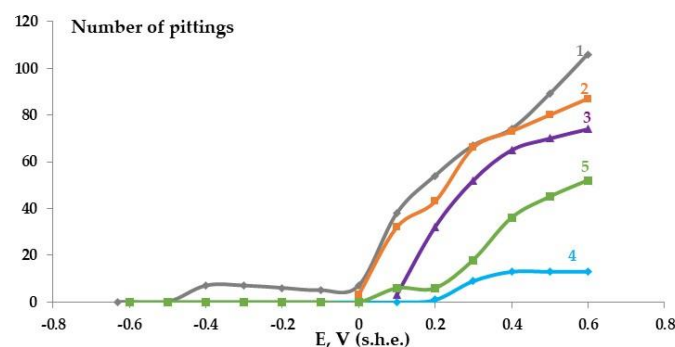


Figure 7. Effect of anodic potential on the development of the pitting dissolution of carbon steel. 1—non-modified steel, 2—steel modified with a VS solution; 3—steel modified with an AS solution; 4—steel modified with a solution of a (VS + BTA) mixture; 5—steel modified with a solution of a (VS + AS) mixture. Conditions of recording the anodic polarization curve (Figure 3): 0.1 M solution NaCl. Potential scan rate: 1 mV/s.

Apparently, at potentials close to E_{pit} , metastable pits [31,37] are formed on the surface and quickly re-passivated. The simultaneous appearance/disappearance of pits occurs on the surface at these potentials. Apparently, stable pits begin to form at potentials above +0.2 V.

Preliminary modification of the steel surface with formulations based on organosilanes leads to inhibition of metal pitting dissolution, i.e., at equal potentials, fewer pits are observed on the surface (Figure 7). Modification of the surface with a solution of (VS + BTA) and (VS + AS) mixtures inhibits pitting dissolution most efficiently. In addition, the effect of modification of the carbon steel surface with organosilanes on the pit formation at a constant anodic potential was studied.

Figure 8 shows the kinetic curves of the development of anodic pitting dissolution (pit formation) on carbon steel. It was found that the first pits occur on the surface after 10 min of polarization, and preliminary modification of the steel surface with solutions of individual silanes (not mixtures!) does not provide satisfactory inhibition of local anodic dissolution of the metal. For example, the use of a modifying solution based on vinylsilane (VS) nearly did not affect the pit formation on steel (Figure 8, curves 1, 3). In the initial polarization period (10 min), the number of pits formed on the samples previously modified with a VS solution was slightly smaller than that on non-modified metal (comparison of curves 1 and 3, Figure 8, i.e., 69 and 78 pit/cm² for non-modified steel and after steel modification with the VS solution, respectively). It has been shown that during the entire test, the number of pits on the metal surface modified with an AS solution was almost the same as on the non-modified surface (Figure 8, curves 1, 3). Preliminary surface modification with a solution of the amino-containing silane (AS) led to inhibition of pit formation for the first 60 min of testing, namely, the number of pits formed on the non-modified surface was more than twice the number of pits on the surface modified with AS (Figure 8, curve 2). However, in longer tests (more than 60 min), the difference in the number of pits formed on modified and non-modified surfaces decreased but almost leveled off after 120 min of testing: 96 and 90 pit/cm² for non-modified and AS-modified steel, respectively. It was shown in our previous studies [38,39] that the use of organosilanes in a mixture with an organic corrosion inhibitor, in particular with the well-known [40] nitrogen-containing inhibitor, 1,2,3-benzotriazole (BTA), leads to a significant increase in inhibitory efficiency, which in the case of the mixture significantly exceeded the efficiency of each component alone. Modification of steel surface with a solution of a mixture of vinylsilane and BTA provided the most efficient inhibition of local dissolution of the metal (Figure 8, curve 4). In this case, the number of pits formed after 120 min of testing (under potentiostatic conditions at $E = +0.2$ V) in the chloride-containing solution on the non-modified steel surface was almost twice as large as the number of pits on steel modified with a mixture solution (VS + BTA): 96 and 39 pits on non-modified and modified metal, respectively.

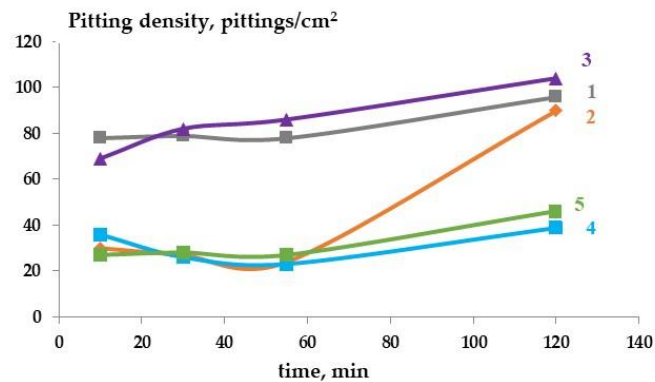


Figure 8. Kinetics of pit formation on carbon steel under potentiostatic polarization. 1—non-modified steel, 2—steel modified with a VS solution; 3—steel modified with an AS solution; 4—steel modified with a solution of a (VS + BTA) mixture; 5—steel modified with a solution of a (VS + AS) mixture. $E = +0.2$ V, borate buffer with addition of 0.1 M NaCl, pH 6.9.

Corrosion tests of metals modified with formulations based on organosilanes performed in the corrosive chloride-containing electrolyte showed that organosilicon surface nanolayers inhibited the corrosion of steel. In fact, accelerated tests conducted in the climate chamber at $T = 60$ °C and RH = 95% showed inhibition of atmospheric corrosion with organosilicon surface nanolayers. Figure 9 shows photos of zinc samples modified with formulations based on organosilanes after two months of testing.

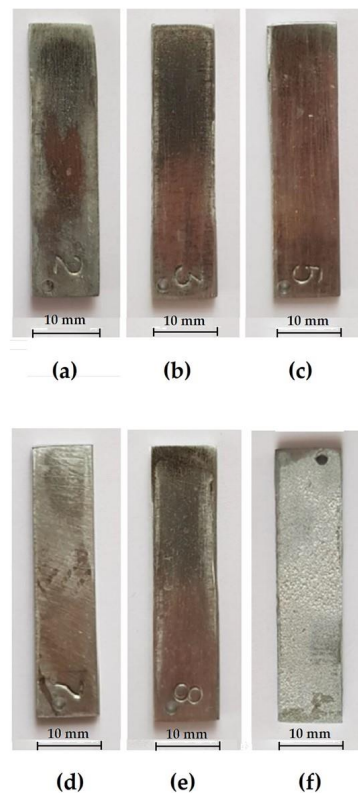
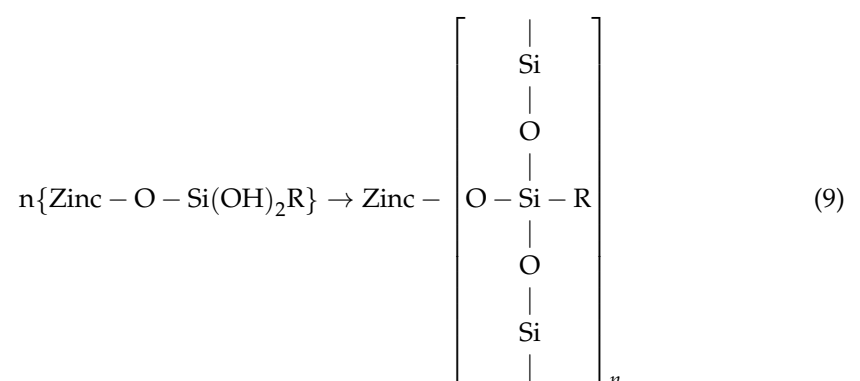
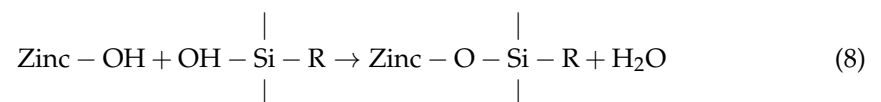


Figure 9. Appearance of zinc samples modified with formulations based on organosilanes after accelerated corrosion tests in the climate chamber, (a)—non-modified metal; zinc modified with: (b)—1% aqueous solution of VS; (c)—aqueous solution of (1% VS + 1% AS) mixture; (d)—neutral 1% aqueous solution of GS; (e)—neutral 1% aqueous solution of AS; (f)—acid 10% aqueous solution of GS with addition of acetic acid (pH 4.0), $T = 60$ °C, RH = 95%, test duration 60 days.

It was found that after two months of accelerated atmospheric corrosion tests, a thin layer of white corrosion products occupying approximately 20% of the sample surface area was present on the surface of non-modified zinc (Figure 9a).

After preliminary modification of the surface with the VS solution, the degree of surface coverage with corrosion products decreased to 10%. Surface modification with aqueous neutral solutions of AS and GS (Table 2, lines 8, 18) hardly affected the amount of corrosion products on the surface: 19 and 23% of the surface was covered with corrosion products in the case of AS and GS, respectively. The use of acid rather than neutral silane solution for modification (modifying solution with addition of acetic acid, Table 2, line 19) led to the formation of a “thick” surface organosilicon film with a thickness of 126 μm . It is known that the following reactions occur more intensely and completely in acid solutions: alkoxy silane hydrolysis reactions to give an organosilanol (reaction (7)), condensation of organosilane silanol groups and hydroxyl groups of the metal surface with formation of covalent Me-O-Si bonds (reaction (8)), and polycondensation of adjacent silanol groups with formation of a surface siloxane polymer (reaction (9)) [41–44].



Apparently, an external three-dimensional reticular siloxane layer growing in thickness formed on the surface if the acidified modifying solution was used. However, during the first day of testing, this “thick” film spontaneously peeled off from the sample surface. Moreover, after 2 months of accelerated testing, after peeling of the “thick” siloxane film, the entire surface of the sample (100%) was covered with corrosion products (Figure 9e). It can be assumed that in case of modifying with acidified solution, a two-layer film formed on the surface: a thin (nanosized) 2D layer of linear siloxane polymer molecules closer to the surface, and above it, an external “thick” (30–40 μm thick) 3D reticular layer. It could be expected that the outer reticular layer would prevent the penetration of corrosive medium components to the surface and hence inhibit corrosion. The layer closer to the surface consists of linear non-cross-linked siloxane molecules that do not provide the surface shielding required for corrosion inhibition. The corrosion process occurs intensely in the areas that are not occupied by the siloxane layer. Furthermore, considering that corrosion products have a larger volume, the entire surface is covered with corrosion products. The absence of cross-links between linear chains of siloxane molecules in the layer closest to the surface is probably caused by diffusion limitations. They probably also account for the weak adhesion between the outer and inner layers which causes fast delamination of the outer layer under the influence of humidity and temperature.

Figure 10 and Table 4 show the corrosion rates of zinc samples after accelerated corrosion tests in the climatic chamber in a chloride-containing solution determined gravimetrically.

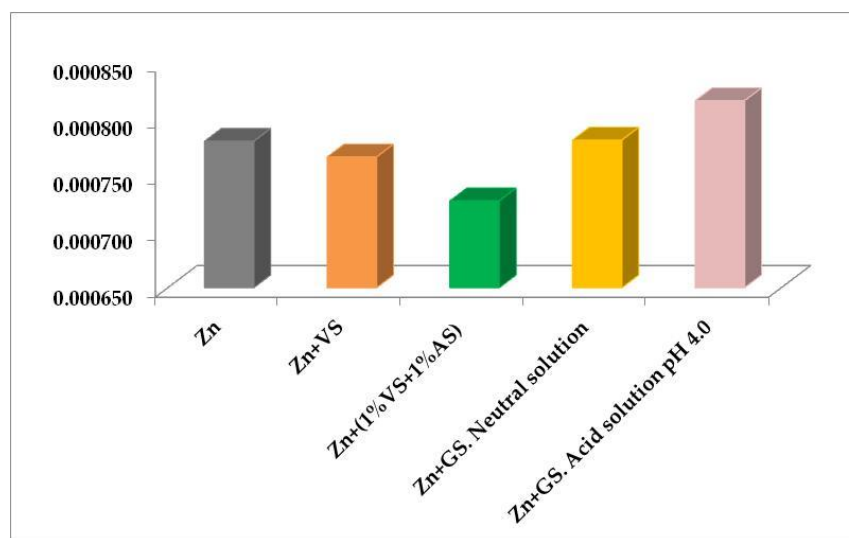


Figure 10. Effect of metal surface pre-modification with formulations based on organosilanes on the corrosion of zinc in the electrolyte. Accelerated corrosion tests in 0.1 M sodium chloride solution. Test duration: 66 days. Corrosion rates were determined by the gravimetry method.

Table 4. Effect of preliminary modification of the metal surface with formulations based on organosilanes on the atmospheric corrosion of zinc. Accelerated corrosion tests, climate chamber, $T = 60\text{ }^{\circ}\text{C}$; RH = 95%. Tests duration: 51 days. Corrosion rates were determined by the gravimetry method.

System	Corrosion Rate, Micrometers Per Year
Unmodified Zn	0.02609
Zn + VS	0.01806
Zn + (1% VS + 1% AS)	0.01672
Zn + GS. Neutral solution	0.02241
Zn + GS. Acid solution pH 4.0	1.72849

It can be seen from the test results that the preliminary modification of metal surface with solutions of individual silanes slightly affects the uniform corrosion of zinc. Moreover, modification of the surface with an acidified GS solution, which ensures the formation of a “thick” film that peels off from the surface after 1 day of testing, activates corrosion, i.e., the corrosion rate increases compared to that of the non-modified metal. Modification of the surface with neutral VS and GS solutions reduced the rate of zinc corrosion quite insignificantly, namely 1.4- and 1.1-fold for VS and GS, respectively. Modification of the surface with an acidified GS solution, which led to the formation of a 126 μm thick film that peeled off from the surface during the first day of testing, accelerated zinc corrosion; in this case, the corrosion rate even slightly exceeded the value found for the non-modified metal (Table 4). Apparently, after the majority of the siloxane film peeled off, a thin defective siloxane film remained on the surface. The dissolution of the metal (anodic reaction) occurred from the film defects on a relatively small area, i.e., the anodic sites. In contrast, the area of the cathodic sites where reduction of oxygen as a depolarizer of the corrosion process occurs (the cathodic reaction) is rather large. In addition, since the total rates of cathodic and anodic corrosion reactions are equal, an increase in the rate of the cathodic reaction of oxygen reduction should cause an increase in the metal dissolution rate. Therefore, one could expect higher dissolution rates from the “anodic” defects, which provides an increase in the mean corrosion rate as determined gravimetrically. The corrosion rate dropped one and a half times after surface modification with a solution comprising a mixture of VS and AS, as was expected for the reasons outlined above. Thus,

modification of the metal surface with individual organosilane solutions does not result in a reduction in the rate of atmospheric corrosion of the metal, which can be accomplished with a modifying solution based on a mixture of vinyl- and aminosilanes. Figure 10 shows the effect of surface modification on the corrosion of zinc in a chloride-containing solution.

It has been shown that the corrosion rate of non-modified zinc in the chloride-containing solution is low and amounts to 0.78 $\mu\text{m}/\text{year}$ (Figure 10) and that the preliminary modification of the zinc surface does not significantly affect the corrosion behavior of the metal (Figure 10). In fact, modification with solutions of individual silanes practically does not change the corrosion rate of zinc significantly, and if the acidified modifying GS solution was used, even a slight increase in the corrosion rate (0.81 $\mu\text{m}/\text{year}$) was observed. A small inhibition of zinc corrosion was noted upon modifying the surface with a solution of a mixture of vinyl- and aminosilanes: the corrosion rates were 0.78 and 0.73 $\mu\text{m}/\text{year}$ for non-modified zinc and zinc modified with a mixture of VS and AS, respectively. Thus, the results of polarization and corrosion studies show that the organosilicon surface layers formed upon modification with formulations with solutions based on organosilanes are capable of increasing the passivating ability, inhibiting local anodic dissolution and atmospheric corrosion of metals, and inhibiting corrosion in corrosive electrolytes. Binary modifiers, namely a mixture of vinyl- and aminosilanes and a mixture of vinylsilane and benzotriazole, favor the inhibition of metal corrosion most efficiently.

Preliminary modification of the surface can have a decisive influence not only on the atmospheric corrosion of zinc, but also of other metals. In our previous work, we studied the effect of organosilicon surface layers on the atmospheric corrosion of iron and carbon steel and showed the inhibition of atmospheric corrosion of metal [17].

Additional information about the protective effect provided by modifying the steel surface with silane solutions was obtained using EIS. The equivalent circuit (EC) used to interpret the EIS results consists of electrical elements corresponding to the probable physical processes occurring in the system under study, i.e., “non-modified metal/silane-modified metal—corrosive medium”. As a rule, these elements include resistance and capacitance [42].

In this study, two ECs (Figure 11a,b) in which the capacitive elements were replaced by constant-phase elements (CPE) were used to process the results. The spectra obtained were compared with the impedance of the selected ECs using complex nonlinear approximation programs DCS [28]. R_0 is the resistance of the electrolyte between the test sample (the working electrode) and Luggin’s capillary of the reference electrode (Figure 2). Its value depends on the solution conductivity and the distance between the sample surface and the capillary. R_p is the charge-transfer reaction resistance that determines the kinetics of the corrosion process, so this parameter was used to estimate the effect of surface modification in accordance with the Formula (10):

$$K = k \cdot (1/R_p) \quad (10)$$

where K is the metal corrosion rate, R_p is the charge-transfer reaction resistance, and k is a proportionality coefficient.

In the EC presented in Figure 10b, R_1 is the sum of the resistances of the oxide/hydroxide surface layers and the silane layer. Unlike the classical ECs [45], the use of CPE elements instead of capacitances makes it possible to more accurately simulate experimental data and obtain additional information about the nature of electrode processes. The CPE impedance was described by the Equation (11) [41].

$$Z_{\text{CPE}} = A^{-1} (j \omega)^{-n} \quad (11)$$

where A is a coefficient (modulus);

j is the imaginary unit; ω is the cyclic frequency; and n is the phase coefficient.

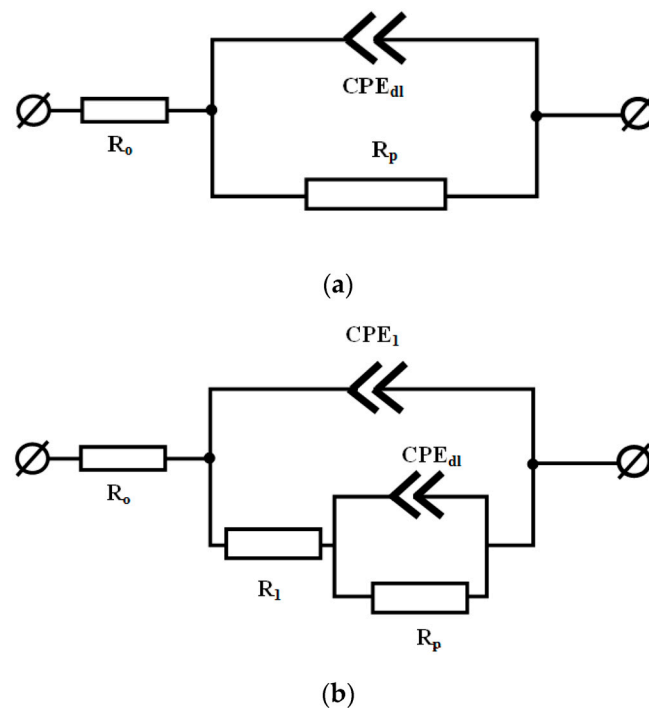


Figure 11. Equivalent circuits used to fit impedance data. For non-modified steel (a) and steel pre-modified with organosilanes solutions (b).

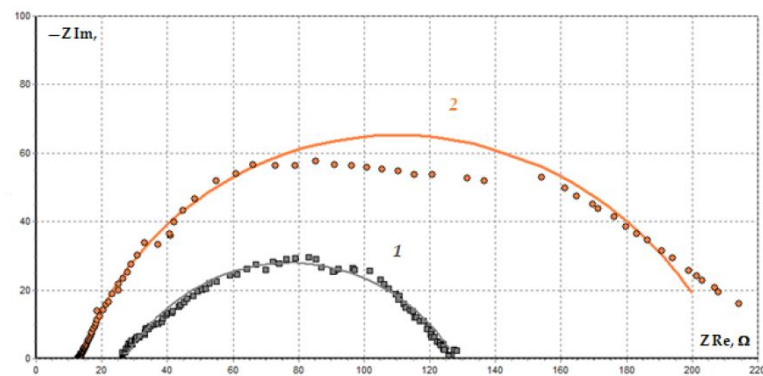
Depending on the value of the phase coefficient, the CPE element can be interpreted as an ideal capacitor ($n = 1$), or a resistor ($n = 0$). As for the selected ECs (Figure 11a,b), the value of the phase coefficient that differs from unity can be used to assess how perfect the simulated capacitance is and how uniform the capacitor plates are.

In the equivalent circuits (Figure 10a,b) used to simulate the obtained results, the CPE1 element characterizes the capacitance of the metal-electrolyte interface and mainly depends on the structure of the surface layers, and the CPEdl element reflects the capacitance of the electrical double layer in the Faraday process.

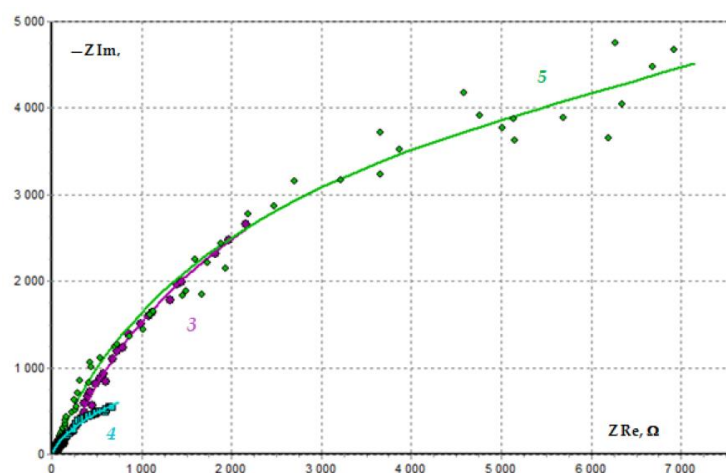
In equivalent circuits used to simulate the results obtained, the Nyquist plots of steel before and after modifying with silanes are shown in Figure 12.

The resulting arc on the Nyquist plot is described by a single $R_p/CPEdl$ chain and is related to the kinetics of the Faraday process (i.e., charge transfer) on the metal, which actually determines the corrosion behavior of the steel. After modifying the samples in all the studied systems, the hodographs show a more complex shape (Figure 12a,b); therefore, the following EC (Figure 11b) was used to describe them, which consists of two parallel R/CPE chains. The high-frequency region on the Nyquist plot in the selected model corresponds to the time constant, mainly associated with the $R_1/CPE1$ chain, i.e., it depends on the conductivity of the surface layer (Figure 12c). The nature of the low-frequency region is similar to $R_p/CPEdl$ described above for the circuit in Figure 11a.

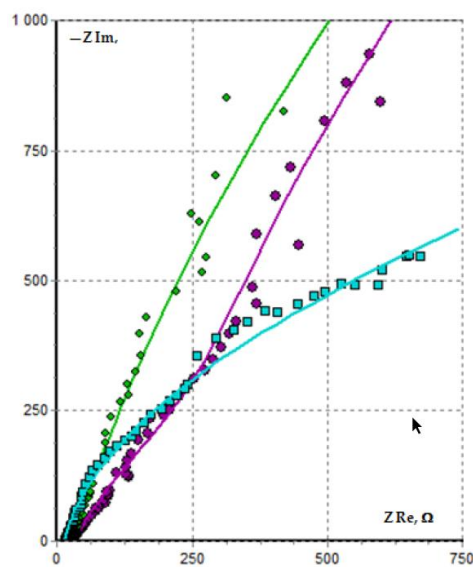
In the case of non-modified steel (Figure 11a), the Nyquist plot is represented by only one semicircle that is simulated by an EC (Figure 10a). The arc in the Nyquist plot is related to the kinetics of the Faraday process (i.e., charge transfer) on the metal, which actually determines the corrosion behavior of steel. After modifying the samples in all the systems studied, the Nyquist and Bode plots demonstrated a more complex shape (Figure 12b,c), therefore the second EC was used to simulate them (Figure 11b). The capacitive circuit in the high-frequency area is a process of electric charge transfer described by the R_p/CPE circuit as part of the overall equivalent circuit. The values of the elements obtained by calculations are presented in Table 5. The simulation error did not exceed 5% in all cases.



(a)



(b)



(c)

Figure 12. Nyquist plots of steel electrode: (a) before modifying (1) and after modifying the surface with 1% VS (2); (b) with 1% AS (3), 1% VS + 1 mM BTA (4) and 1% VS + 1% AS (5); (c) increased high frequency section. (Comparison between measured and simulated spectra. Dotted lines represent measured spectra and solid lines represent simulated spectra).

Table 5. Parameters of equivalent circuits used for simulation of EIS results on steel in solution (0.4 M H₃BO₃ + 5.5 mM Na₂B₄O₇ × 10H₂O, pH 6.7 with the addition of 0.1 M NaCl.

System	R_0 , kΩ·cm ²	R_1 , kΩ·cm ²	CPE1 A, S·s ⁿ /cm ²	CPE1 n	R_p , kΩ·cm ²	CPE _{dl} A, S·s ⁿ /cm ²	CPE _{dl} n
Non-modified St 3	26	-	-	-	101	45 × 10 ⁻⁵	0.64
1% VS	13	195	77 × 10 ⁻⁵	0.70	187	6.4 × 10 ⁻⁵	1
1% AS	30	1339	29 × 10 ⁻⁵	0.69	10,572	7.4 × 10 ⁻⁵	1
1% VS + 1 mM BTA	16	607	35 × 10 ⁻⁵	0.84	2138	6.9 × 10 ⁻⁵	0.69
1% VS + 1% AS	30	6196	55 × 10 ⁻⁵	0.81	12,440	7.6 × 10 ⁻⁵	0.73

From Figure 12, it can be seen that the radii of the arcs on the Nyquist plots obtained on modified samples are significantly larger than those on the non-modified metal. The calculated R_p values can be used to estimate the effect of surface modification with silanes on the corrosion process. The inhibition coefficient of the electrochemical reaction of metal ionization (corrosion) by layers obtained as a result of surface modification (γ) can be determined as the ratio of charge transfer resistances for the modified (R_p^{sil}) and non-modified (R_p^{none}) samples (12):

$$\gamma = R_p^{\text{sil}} / R_p^{\text{none}} \quad (12)$$

The calculated inhibition coefficients for the modifying formulations studied are given in Table 6:

Table 6. Values of corrosion inhibition coefficients of steel with modifying formulations.

System	1% VS	1% VS + 1 mM BTA	1% VS + 1% AS	1% AS
γ	1.85	21.2	123.2	104.7

Based on the results obtained, it can be concluded that the corrosion of carbon steel is inhibited most efficiently by the organosilicon layer obtained by modifying the surface with solutions containing aminosilane and a mixture of vinyl- and aminosilanes.

However, in a comprehensive assessment of the results of modification, one should take into account the significance of other EC parameters, which can serve as additional evidence of an inhibitory effect. Thus, a comparison of the resistance values of the surface layer of the sample after modification R_1 (Table 3) for 1% VS and 1% AS shows an increase in this parameter by seven times, and for the sample after modification with a mixture of 1% BC + 1% AS, this value increases by 32 times, while a mixture of 1% VS + 1 mM BTA gives an increase of only three times. However, it should be noted that the phase coefficient CPE1 for this mixture is maximum: $n = 0.84$ (Table 3). This characterizes the steel surface after inoculation with binary mixtures as more uniform in structure. Then, the studied modifying compositions according to their inhibitory effectiveness can be arranged in the following row:

$$1\% \text{ VS} < 1\% \text{ AS} < (1\% \text{ VS} + 1 \text{ mM BTA}) < (1\% \text{ VS} + 1\% \text{ AS})$$

Therefore, the results of EIS studies confirm the conclusions drawn from the above results of corrosion tests and electrochemical studies, i.e., the most efficient inhibition of metal ionization was observed in the case of binary modifying formulations: solutions of the (BC + AS) and (VS + BTA) mixtures. The reasons for such efficiency of binary mixed formulations are considered below.

The formulations containing aminosilane manifest high efficiency because the amino group is a catalyst for silane hydrolysis (reaction (7), condensation of organosilane silanol groups and hydroxyl groups on the metal surface (with formation of covalent Me-O-Si

bonds (reaction (8)), and polycondensation of adjacent silanol groups (with formation of a surface siloxane polymer (reaction (9))). In addition, aminosilane demonstrates a self-catalytic effect when it binds to the surface and forms a surface siloxane layer [46]. Moreover, to obtain densely cross-linked branched (reticular) polymer layers firmly bound to the surface, it is recommended to add a small amount of aminosilane to the modifying solution and use neutral organosilanes mixed with amino-containing silane [47]. Earlier, we have shown that introducing a mixture of amino- and vinyl-containing silanes into a polymer coating leads both to an increase in the adhesion of the coating and to the inhibition of stress corrosion cracking of pipe steel [42].

As for the modifying formulation, i.e., the mixture of VS and benzotriazole, it was previously shown in the literature [17,19,43–45] that the use of organosilanes in a mixture with organic corrosion inhibitors, with benzotriazole in particular [38], increases the inhibitory efficiency significantly, which considerably exceeded the efficiency of each of the mixture components alone. We have made an addition to the article regarding the characterization of surface layers:

In our previous works [38–40], the surface layer formed by modifying the metal surface with a mixture of benzotriazole and organosilane was characterized in detail using modern techniques for surface investigation: Fourier-Transform Infrared spectroscopy (FT-IR), X-ray photoelectron spectroscopy (XPS), Scanning Electron Microscopy with Energy Dispersive Spectroscopy (SEM-EDS), and X-ray spectral microanalysis (XSMA). The application of these methods made it possible, with a high degree of reliability, to detail the processes occurring on the metal surface during the interaction of organosilane with it and to propose a diagram of the structure of the interface shown in Figure 13. Nitrogen-containing benzotriazole, like other organic amines, can act as a catalyst for condensation reactions of the silanol group ((8), (9)), making these reactions occur more fully and, as a consequence, providing the formation of a denser cross-linked reticular siloxano-azole surface nanolayer (Figure 13) [38] that hinders the access of corrosive medium components (oxygen, water, electrolyte anions) to the surface.

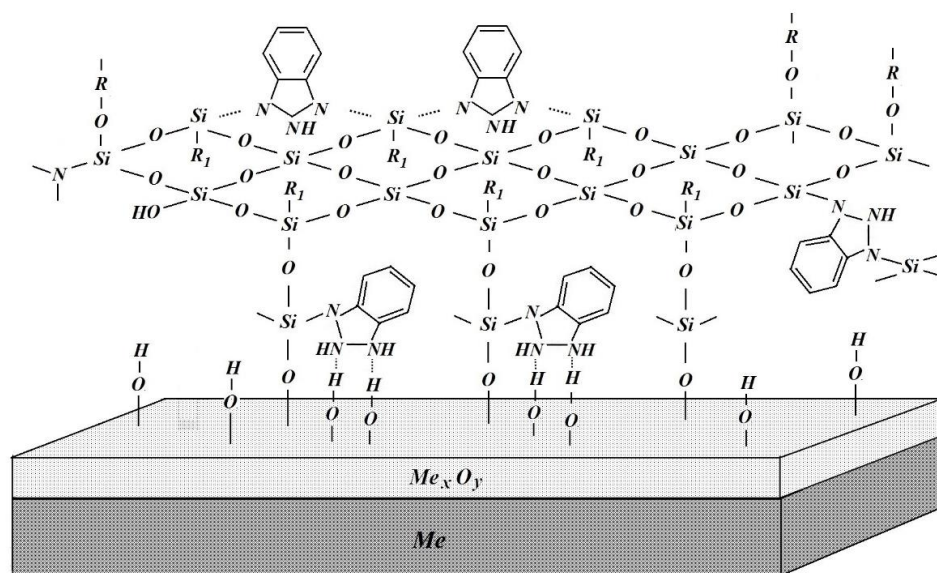


Figure 13. Structure of a siloxano-azole nanolayer on carbon steel surface.

The results of impedance measurements are presented in Table 5. From Table 5, it can be seen that non-modified steel has a relatively low polarization resistance (not exceeding 100 Ohm) of steel corrosion. Preliminary modification of the metal surface with a vinylsilane solution provided an insignificant increase in polarization resistance and inhibition of steel corrosion, whereas the capacitance even increased (see Table 5), apparently due to the porosity of the vinyl siloxane surface layer that consists of linear

oligomeric chains and does not prevent the access of electrolyte components to the metal surface. The use of the amino-containing silane led to a significant (more than by an order of magnitude) increase in polarization resistance, which might be caused by the formation of a more tightly crosslinked reticular polymer-oligomeric surface nanolayer comprising not only linear chains, but also cross-links. This may occur because the amino group is a catalyst for the hydrolysis of alkoxysilanes ($-\text{Si-OAlk}$) and formation of silanols ($-\text{Si-OH}$) (reaction (7)), condensation of organosilane silanol groups and hydroxyl groups on the metal surface (with the formation of covalent Me-O-Si bonds, reaction (8) and polycondensation of adjacent silanol groups (with formation of a surface siloxane polymer, reaction (9)). Moreover, aminosilane demonstrates a self-catalytic effect as it binds to the surface and forms a surface siloxane layer [46]. To obtain cross-linked branched (reticular) polymer layers strongly bound to the surface, it is recommended to add a small amount of aminosilane to the modifying solution and use neutral organosilanes mixed with amino-containing silane [47]. Earlier we have shown that incorporation of a mixture of amino- and vinyl-containing silanes into a polymer coating leads both to an increase in the coating adhesion and to the inhibition of stress corrosion cracking of pipe steel [42].

The greatest increase in the polarization resistance of steel was observed after surface modification with solutions of mixed formulations: mixtures of VS and benzotriazole and, especially, mixtures of VS and AS (Table 3). It has previously been shown in the literature [17,19,38,39] that the use of mixture of amino- and vinylsilanes [42] and mixtures of organosilanes with organic corrosion inhibitors (in particular, with benzotriazole [38]) leads to a significant increase in inhibitory efficiency, which significantly exceeded the efficiency of each of the mixture components. In addition, nitrogen-containing benzotriazole, similarly to organic amines, can act as a catalyst for condensation reactions of the silanol group ((7), (8)), causing the reactions to occur more completely and, as a result, provide the formation of a denser and better cross-linked reticulate siloxano-azole surface nanolayer whose structure is shown in Figure 13, restricting the access of corrosive components of the medium (oxygen, water, electrolyte anions) to the surface.

4. Conclusions

1. Methods for the preliminary modification of the surface of structural metals with formulations based on organosilanes, including both solutions of individual organosilanes and two-component mixtures consisting of two organosilanes or an organosilane with an organic corrosion inhibitor, have been developed. Such a modification creates self-organizing siloxane polymer/oligomeric layers on the metal surface.
2. These layers are capable of changing the physicochemical properties of the metal surface, in particular, reducing the metal's susceptibility to corrosion degradation.
3. It has been found that organosilicon surface films can increase the passivating ability of metals, inhibit local anodic dissolution of steel and atmospheric corrosion of zinc, and hinder the corrosion of zinc in corrosive electrolytes.
4. Surface layers formed by binary modifiers, namely mixtures of vinyl- and aminosilanes and mixtures of vinylsilane and benzotriazole, inhibit the corrosion of metals most effectively.
5. The mechanism of corrosion inhibition by surface nanolayers formed upon surface modification by two-component mixtures has been considered.

Author Contributions: Conceptualization, project administration, visualization, supervision, writing—original draft preparation, writing—review and editing: M.P.; methodology, formal analysis, funding acquisition, resources, data curation: T.Y.; investigation, software, validation, writing—review and editing, impedance investigations: A.R.; methodology, conceptualization, formal analysis, funding acquisition, writing—original draft preparation: L.M. All authors have read and agreed to the published version of the manuscript.

Funding: This research was carried out within the state assignment of the Ministry of Science and Higher Education of the Russian Federation (theme No. 122011300078-1).

Data Availability Statement: Not applicable.

Conflicts of Interest: The authors declare no conflict of interest.

References

1. McCafferty, E. *Introduction to Corrosion Science*; Springer Science + Business Media: New York, USA, 2010; p. 565.
2. Sastri, V.S. *Challenges in Corrosion: Costs, Causes, Consequences and Control*; John Wiley & Sons Ltd.: Hoboken, NJ, USA, 2015; p. 408.
3. *The Cost of Corrosion in China*; Science Press-Springer: Beijing, China, 2018; p. 941.
4. *Trends in Oil and Gas Corrosion Research and Technologies*; El-Sherik, A.M. (Ed.) Woodhead Publishing: Cambridge, UK, 2017; p. 890.
5. Vogelsang, J.A. Anticorrosive pigments in organic coatings. In *Self-Healing Properties of New Surface Treatments*; Fedrizzi, L., Furbeth, W., Montemor, F., Eds.; Maney Publishing: Leeds, UK, 2011; pp. 1–11.
6. *White Paper Strategy for a Future Chemical Policy of the Commission of the European Communities*; Commission of the European Communities Ed.: Brussels, Belgium, 2001.
7. Leuenberger-Minger, A.U.; Faller, M.; Richner, P. Runoff of copper and zinc caused by atmospheric corrosion. *Mater. Corros.* **2002**, *53*, 157–164. [[CrossRef](#)]
8. Leygraf, C.; Wallinder, I.O.; Tidblad, J.; Graedel, T. *Atmospheric Corrosion*, 2nd ed.; John Wiley & Sons: New Haven, CT, USA, 2016; p. 470.
9. Knudsen, O.O.; Forsgren, A. *Corrosion Control through Organic Coatings*, 2nd ed.; CRC Press: London, UK, 2017; p. 256.
10. Bierwagen, G.P. *Organic Coatings for Corrosion Control*; American Chemical Society: Washington, DC, USA, 1998; p. 2.
11. De Graeve, I.; Vereecken, J.; Franquet, A.; Van Schaftinghen, T.; Terryn, H. Silane Coating of Metal Substrates: Complementary Use of Electrochemical, Optical and Thermal Analysis for the Evaluation of Film Properties. *Prog. Org. Coat.* **2007**, *59*, 224–229. [[CrossRef](#)]
12. Twite, R.L.; Bierwagen, G.P. Review of Alternatives to Chromate for Corrosion Protection of Aluminum Aerospace Alloys. *Prog. Org. Coat.* **1998**, *33*, 91–100. [[CrossRef](#)]
13. Dodds, P.C.; Williams, J.; Radcliffe, G. Chromate-free Smart Release Corrosion Inhibitive Pigments Containing Cations. *Prog. Org. Coat.* **2017**, *102*, 107–114. [[CrossRef](#)]
14. Wang, W.-J.; Liu, J.; Liu, X.-F.; Li, Q.-W. Electrodeposited Chromate-Free Organic Passive Film on the Rolled Copper Foil. *Prog. Org. Coat.* **2022**, *63*, 106663. [[CrossRef](#)]
15. Pocius, A.V. *Adhesion and Adhesives Technology: An Introduction*, 3rd ed.; Hanser Publications: Munich, Germany, 2012; p. 198.
16. *Adhesion Aspects of Polymeric Coating*, 2nd ed.; Mittal, K.L. (Ed.) Springer: Boston, MA, USA, 2011; p. 657.
17. Petrunin, M.A.; Gladkikh, N.A.; Maleeva, M.A.; Maksaeva, L.B.; Yurasova, T.A. The Use of Organosilanes to Inhibit Metal Corrosion. A review. *Int. J. Corr. Scale Inhib.* **2019**, *8*, 882–907.
18. Mäkinen, E.; Lassila, L.; Varrelä, J.; Vallittu, P. Light-Curing of Orthodontic Bracket Adhesive by Transillumination through Dentine and Enamel. *Biomater. Investig. Dent.* **2019**, *6*, 6–12. [[CrossRef](#)] [[PubMed](#)]
19. Wang, D.; Bierwagen, G.P. Sol–Gel Coatings on Metals for Corrosion Protection. *Prog. Org. Coat.* **2009**, *64*, 327–338. [[CrossRef](#)]
20. Naihzad, A.S.; Rostam, R.A.M.; Kardar, P.; Feder, M. Active Corrosion Performance of Magnesium by Silane Coatings Reinforced with Polyaniiline/Praseodymium. *Prog. Org. Coat.* **2020**, *140*, 1055046.
21. Matinlinna, J.P.; Lassila, L.V.; Dahl, J.E. Promotion of Adhesion Between Resin and Silica-coated Titanium by Silane Monomers and Formic Acid Catalyst. *Silicon* **2010**, *2*, 87–93. [[CrossRef](#)]
22. Revie, R.W. *Uhlig's Corrosion Handbook*, 3rd ed.; John Wiley & Sons, Inc.: Pennington, NJ, USA, 2011; p. 20111253.
23. Garmanov, M.E.; Kuznetsov, Y.I. Effect of the Scan Rate on the Kinetic Parameters of Active Dissolution and Passivation of Iron in a Neutral Solution. *Prot. Met.* **2004**, *40*, 31–40. [[CrossRef](#)]
24. Kuznetsov, Y.U.I.; Garmanov, M.E. Kinetic Effects of Anions on the Anodic Dissolution and Initial Passivation Steps of Iron in Neutral Borate Solutions. *Elektrokhimiya* **1987**, *23*, 349–354.
25. Marshakov, A.I.; Rybkina, A.A.; Maksaeva, L.B.; Petrunin, M.A.; Nazarov, A.P. A Study of the Initial Stages of Iron Passivation in Neutral Solutions Using the Quartz Crystal Resonator Technique. *Prot. Met. Phys. Chem. Surf.* **2016**, *52*, 936–946. [[CrossRef](#)]
26. *Analytical Methods in Corrosion Science and Engineering*; Marcus, P.; Mansfeld, F. (Eds.) CRC Press-Taylor & Francis Group: Boca Raton, FL, USA, 2006; p. 761.
27. Macdonald, D.D. The history of the Point Defect Model for the passive state: A brief review of film growth aspects. *Electrochim. Acta* **2011**, *56*, 1761–1772. [[CrossRef](#)]
28. Shehrbakov, A.I.; Korosteleva, I.G.; Kasatkina, I.V.; Kasatkin, V.E.; Kornienko, L.P.; Dorofeeva, V.N.; Vysotskii, V.V.; Kotenev, V.A. Impedance of an Aluminum Electrode with a Nanoporous Oxide. *Prot. Met. Phys. Chem. Surf.* **2019**, *55*, 689–694. [[CrossRef](#)]
29. Baboian, R. *Corrosion Tests and Standards: Application and Interpretation*, 2nd ed.; ASTM Int.: West Conshohocken, PA, USA, 2005; p. 43.
30. Soltis, J. Passivity Breakdown, Pit Initiation and Propagation of Pits in Metallic Materials. *Rev. Corros. Sci.* **2015**, *90*, 5–22. [[CrossRef](#)]
31. Szklarska-Smialowska, Z. *Pitting and Crevice Corrosion, NACE International*; The Corrosion Society: Houston, TX, USA, 2005; p. 6.
32. Kuznetsov, Y.U.I. Physicochemical Aspects of Metal Corrosion Inhibition in Aqueous Solutions. *Russ. Chem. Rev.* **2004**, *73*, 75–87. [[CrossRef](#)]

33. Antropov, L.I. Formal Theory of Organic Corrosion Inhibitors. *Protecion Met.* **1977**, *1*, 323–333.
34. Reshetnikov, S.M.; Krutkina, T.G.; Burmistr, M.V. The interdependence of adsorption and protective properties of acidic-corrosion inhibitors. *Prot. Met.* **1980**, *16*, 173–176.
35. Newman, J.; Balsara, N.P. *Electrochemical Systems*, 3rd ed.; Newman, J.K., Thomas-Alyea, E., Eds.; John Wiley & Sons, Inc.: Hoboken, NJ, USA, 2004; p. 207.
36. Kaesche, H. *Die Korrosion der Metalle: PhysiLalisch-chemische Principien und Aktuelle Probleme*, 2nd ed.; Springer: Berlin/Heidelberg, Germany, 1979; p. 181.
37. Tang, Y.; Zao, Y. The Metastable Pitting of Mild Steel in Bicarbonate Solutions. *Mater. Chem. Phys.* **2004**, *88*, 221–226. [[CrossRef](#)]
38. Gladkikh, N.; Makarychev, Y.; Maleeva, M.; Petrunin, M.; Maksaeva, L.; Rybkina, A.; Marshakov, A.; Kuznetsov, Y. Synthesis of Thin Organic Layers Containing Silane Coupling Agents and Azole on the Surface of Mild Steel. Synergism of Inhibitors for Corrosion Protection of Underground Pipelines. *Prog. Org. Coat.* **2019**, *132*, 481–484. [[CrossRef](#)]
39. Gladkikh, N.; Makarychev, Y.; Petrunin, M.; Maleeva, M.; Maksaeva, L.; Rybkina, A.; Marshakov, A. Synergistic Effect of Silanes and Azole for Enhanced Corrosion Protection of Carbon Steel by Polymeric Coatings. *Prog. Org. Coat.* **2020**, *138*, 105386. [[CrossRef](#)]
40. Petrunin, M.; Maksaeva, L.; Gladkikh, N.; Makarychev, Y.; Maleeva, M.; Yurasova, T.; Nazarov, A. Thin Benzotriazole films for Inhibition of Carbon Steel Corrosion in Neutral Electrolytes. *Coatings* **2020**, *10*, 362. [[CrossRef](#)]
41. Maleeva, M.A.; Ignatenko, V.E.; Shapagin, A.V.; Sherbina, A.A.; Maksaeva, L.B.; Marshakov, A.I.; Petrunin, M.A. Modification of Bituminous Coatings to Prevent Stress Corrosion Cracking of Carbon Steel. *Int. J. Corr. Scale Inhib.* **2015**, *4*, 226–234. [[CrossRef](#)]
42. *Impedance Spectroscopy: Theory, Experiment, and Applications*, 3rd ed.; Macdonald, J.R.; Barsoukov, E. (Eds.) Wiley-Interscience: Chicago, IL, USA, 2016; p. 560.
43. Semiletov, A.M.; Chirkunov, A.A.; Kuznetsov, Y.U.I.; Andreeva, N.P. Improving Steel Passivation with Aqueous Solutions of [3-(2-Aminoethylamino)propyl] trimethoxysilane. *Russ. J. Phys. Chem. A* **2015**, *89*, 2271–2277. [[CrossRef](#)]
44. Shivane, C.; Simhadii, N.B.V.; van Ooij, W.J. Improved water-based silane pretreatment for hot-dip galvanized steel substrates. In *Silane and Other Coupling Agents*; Mittal, K.L., Ed.; CRC Press: Boston, MA, USA, 2007; Volume 4, VSP; pp. 253–275.
45. Samiee, R.; Ramezanzadeh, B.; Mahdavian, M.; Alibakhshi, E. Assessment of the smart self-healing corrosion protection properties of a water-base hybrid organo-silane film combined with non-toxic organic/inorganic environmentally friendly corrosion inhibitors. *J. Clean. Prod.* **2019**, *220*, 340–356. [[CrossRef](#)]
46. Plueddemann, E.P. Bonding Throught Coupling Agents. In *Molecular Characterization of Composite Interfaces*; Ishida, H., Kumar, G., Eds.; Springer Science + Business Media: New York, NY, USA, 1985; pp. 13–24.
47. Abel, M.-L. Organosilanes: Adhesion Promoters and Primers. In *Handbook of Adhesion Technology*; da Silva, L.F.M., Ochsner, A., Adams, R.D., Eds.; Springer: Berlin/Heidelberg, Germany, 2011; pp. 237–258.

Disclaimer/Publisher’s Note: The statements, opinions and data contained in all publications are solely those of the individual author(s) and contributor(s) and not of MDPI and/or the editor(s). MDPI and/or the editor(s) disclaim responsibility for any injury to people or property resulting from any ideas, methods, instructions or products referred to in the content.